Composition and stress of SiGe nanostructures on curved substrates

T. Leontiou[1] and P. C. Kelires[2,3]

[1]*General Department, Frederick University, 1036 Nicosia, Cyprus*

[2]*Research Unit for Nanostructured Materials Systems, Cyprus University of Technology, P.O. Box 50329, 3603 Limassol, Cyprus*

[3]*Department of Mechanical and Materials Science Engineering, Cyprus University of Technology, P.O. Box 50329, 3603 Limassol, Cyprus*

(Received 7 October 2015; revised manuscript received 19 February 2016; published 16 March 2016)

Recent experimental studies of Ge nanoislands on silicon-on-insulator (SOI) substrates have provided a defect-free strain relaxation mechanism through the bending of the substrate. Here, using atomistic Monte Carlo simulations and analytical modeling, we couple this relaxation mechanism with interdiffusion and alloying and observe composition profiles that are completely different from those observed in flat nanoislands. Moreover, for comparable SOI and island thicknesses, intermixing can be greatly reduced and Ge content in the islands is highly preserved.

DOI: 10.1103/PhysRevB.93.125307

I. INTRODUCTION

Various strain relaxation mechanisms affect the properties of heteroepitaxial nanostructures, such as Ge nanoislands grown on Si substrates. The epitaxial strain due to the lattice mismatch between Ge and Si is typically relaxed through plastic deformation (dislocations) and/or through intermixing and alloying, depending on the growth conditions. When the substrate thickness is much greater than that of the deposited film, strain partitioning leaves the substrate with much less strain than that in the film and minimization of the free energy mostly involves the nanoisland region.

However, as the substrate is made thinner, and eventually becomes comparable with the deposited film, energy minimization also affects the substrate. Such is the case of nanoisland formation on silicon-on-insulator (SOI), where Ge is deposited on a thin layer of Si on top of an oxide. It has been demonstrated [1–6] that in this case strain significantly affects the thin Si layer through the introduction of local bending induced by the nanoisland. This behavior is distinctively different from that observed during Ge growth on thick Si substrates. A big advantage is that it leads to defect free structures. Yet, it is totally unknown how local bending affects the island composition and its distribution.

This is crucial to understand for device applications, since it is well known that suitable control of alloying and stress in nanocrystals can be used to modulate their electronic properties [7]. In Si and SiGe, strain provides a mechanism for control of both carrier mobility and band offsets. For example, sufficient biaxial tensile strain can transform Ge into a direct-band-gap material with strongly enhanced light emission efficiency [8].

Here, we study for the first time the effect of curvature on the composition properties of nanostructures, using as a prototype Ge nanoislands on top of a Si (001) substrate. We couple the effect of curvature to that of interdiffusion and demonstrate that the resulting composition profile (CP) significantly differs from that of flat nanoislands, a case which is well studied. We also show that for comparable template and island thicknesses, the Ge content in the islands can be highly preserved as intermixing is slowed down.

II. METHODOLOGY

We study the system at both global equilibrium conditions, as well as at constrained equilibrium (kinetically limited) conditions. The former case corresponds to conditions at which substantial intraisland diffusion and redistribution of the alloy species can take place, [9] such as during growth by the chemical vapor deposition (CVD) method [10,11]. For this case, we use a Monte Carlo (MC) method that has been extensively tested in similar situations [9,12–14]. A deeper understanding is obtained by analytical modeling, coupling the curvature and intermixing effects. The latter case corresponds to conditions at which high diffusion barriers and other geometrical and kinetic factors constrain the diffusion of species at typical growth temperatures. An example of such nonequilibrium conditions is given in the work of Ref. [15], reporting growth by the molecular beam epitaxy (MBE) method. This case is studied by analytical modeling.

In the MC method, the system is allowed to equilibrate, both geometrically and compositionally, by employing three types of random moves: atomic displacements and volume changes, for geometrical relaxation, and mutual identity exchanges between atoms of different kinds, which lead to compositional equilibration and mimic atomic diffusion in the system. The simulations are run in a parallel-processing mode, which speeds considerably the algorithm and allows us to investigate structures similar in size to the ones which are experimentally observed. The energy is calculated using well-established interatomic potentials for Si/Ge [16]. In order to speed up the processes, we initially confined the study to quasi-3D structures, by keeping the thickness in one of the epitaxial dimensions small ($\sim$15 Å). We later on selectively analyzed fully 3D structures and verified that the results obtained are valid. We treat the thin Si template of the SOI structure as if free standing, since the role of the insulator can be ignored to a first approximation [4]. We verified that the structures with the islands on curved SOI substrates are always more stable than the equivalent (having the same amount of Ge) curved conformal 2D configurations on thin Si substrates.

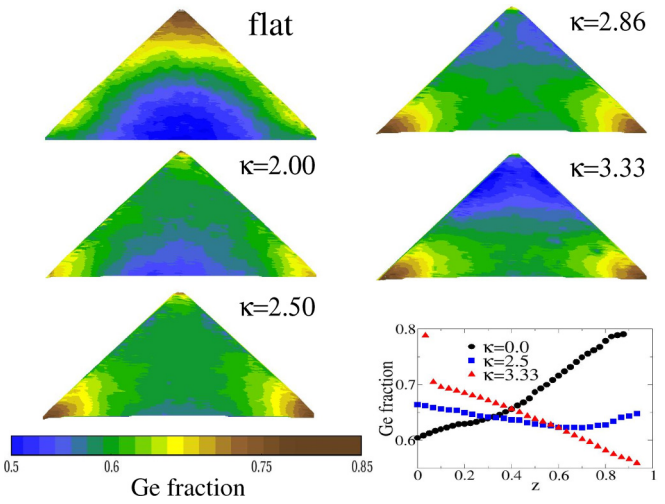

FIG. 1. The equilibrium composition profile at 900 K of a Ge-rich (65% Ge) {111} pyramid for both flat and curved geometries. The units of the curvature κ are 10^{-3} nm^{-1}. The graph shows the Ge fraction, averaged laterally, along the growth direction (in relative units).

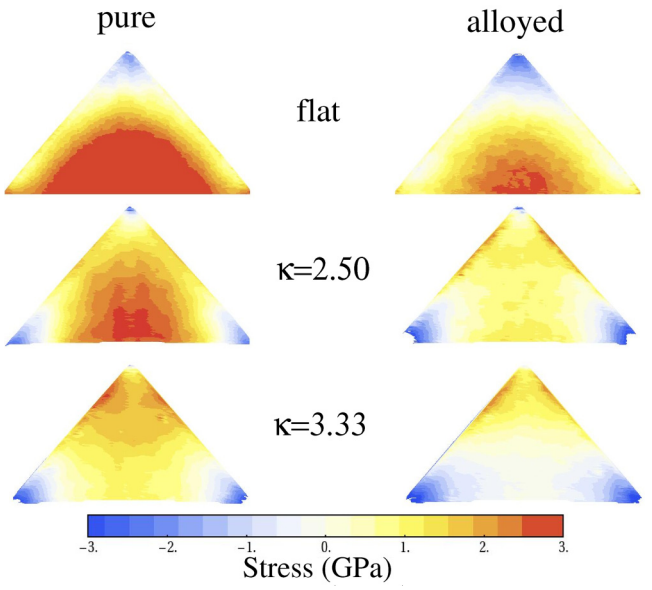

FIG. 2. The stress profile at 900 K of a pure and a 65% Ge alloyed pyramid, for both flat and curved geometries. The units of curvature κ are 10^{-3} nm^{-1}. Stress contours derived from average hydrostatic atomic stresses; sign convention: positive values denote compression, negative values denote tension.

III. RESULTS

A. Shape of composition and stress profiles

We first examine the effect of bending on the shape of the CP of a typical pyramidal nanoisland, having {111} facets and 45° contact angles. The composition in the island is kept fixed at 65% Ge during equilibration. Thus, for the moment, we focus on the island ignoring what happens in the substrate. The results at 900 K, as curvature is gradually increased, are shown in Fig. 1. The flat geometry gives rise to the well established Si-rich core area [9–11], with Ge enriching the periphery and the top. A dramatic change to the CP occurs when curvature κ is introduced. Initially, the Si-rich core is gradually reduced and at a certain value of κ ($\sim 2.86 \times 10^{-3}$ nm for this composition) completely disappears (top right). Notably, this is accompanied by strong segregation of Si to the upper regions of the island and of Ge to the lower ones, especially to the basal corners, forming a radically different CP compared to the flat case. The dramatic reduction of Ge content along the growth direction with increasing curvature is quantified in the accompanying graph. The range of values used for κ is close to what was experimentally observed [1,2], so we expect such CP to be readily extracted by proper techniques (e.g., grazing-incidence XRD or selective etching [17]). Other nanoisland structures on curved substrates, such as shallow angle pyramids or domes exhibit the same dramatic change in shape.

The associated stress profiles for various values of κ are shown in Fig. 2, for both a pure and an alloyed Ge pyramid. In the pure case, curvature reduces the compressive stress in the island core but does not completely eliminate it. Alloying further relaxes the elastic energy and at $\kappa \sim 3.33 \times 10^{-3}$ nm^{-1} the bulk stress is completely neutralized. Although the curved CP shape is very different from the flat CP shape, it can still be largely explained on the basis of elastic energy minimization, i.e., Si accumulating in compressed areas and Ge preferring to accumulate in less compressed areas [9]. We have also verified that the overall shape of the simulated CP, besides some minor changes, remains the same in the temperature range between 300 and 1200 K. This observation indicates and emphasizes that the major driving force behind the formation of the CP is the elastic strain energy.

This new unique CP is not exclusive to the specific Ge composition chosen, but it is global. To demonstrate this, we performed simulations in the semi-grand canonical ensemble [12,13], in which different compositions are generated by varying the chemical potential difference $\Delta\mu$ between Si and Ge. The results, for a fixed curvature, are shown in Fig. 3. We see the same general trend in the shape of the CP, characterized by the segregated areas, at all Ge contents. We expect

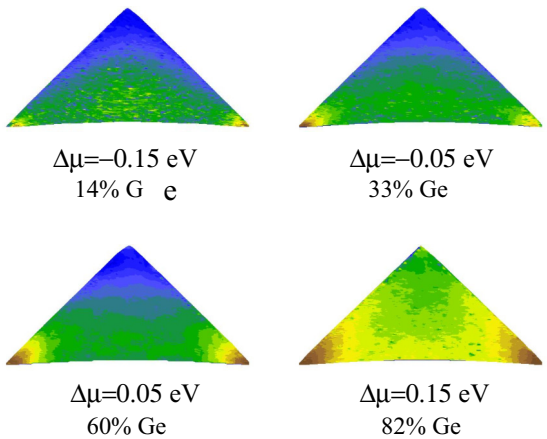

FIG. 3. The composition profile at 900 K for a curved pyramid ($\kappa = 3.33 \times 10^{-3}$ nm^{-1}) for various Ge fractions (obtained in the semi-grand canonical ensemble).

that quantum dots with such CPs may have a significantly different optoelectronic response compared to dots on flat substrates.

B. Thermodynamic model for SOI systems

We now extend our analysis to the whole SOI system (nanoisland plus thin Si template). Our aim is to determine its bending and composition at the same time as a function of the relative thickness of its components. For this, we apply analytical modeling of free-energy minimization. We first start with elastic energy minimization, assuming no alloying between Ge nanoisland and Si template. Under this constrain, the elastic energy is given by [4]

$$U = \frac{C_s}{2}\int_{-ts}^{0} e_s^2 dz + \frac{C_i}{2}\int_{0}^{t_i} e_i^2\left(1-\frac{z}{t_i}\right)^2 dz, \qquad (1)$$

where $e_s = \kappa(z - z_0)$ and $e_i = \kappa(z - z_0) + e_m$ represent the biaxial strain in the substrate and island, respectively. The substrate and island thicknesses are t_s and t_i, while e_m is the misfit strain and z_0 the position of the neutral plane (see Appendix for more details). C_s and C_i are the elastic constants for the substrate and the island.

The induced curvature is derived from Eq. (1) by minimization with respect to κ and z_0. This yields an expression for the curvature that has the form

$$\kappa = -\frac{6\alpha\beta e_m}{t_s}\gamma, \qquad (2)$$

where $\alpha = C_i/C_s$, $\beta = t_i/t_s$ is the ratio of the thicknesses of the two components, and γ is a function of α and β [4]. The values for the induced bending as a function of β predicted by this model are in excellent agreement with the values produced by the MC simulations (see Appendix). This agreement verifies the accuracy of the model in treating the elastic interactions in the system. For more details about this effect, see Refs. [2,4].

The next and crucial step in the study of the composition properties of the whole system is to allow for alloying between the nanoisland and the Si template. This effect can be modeled by expressing the average free energy per atom in the general form

$$F = x(1-x)\Omega + \bar{U} - TS. \qquad (3)$$

The first term describes the chemical energy in the system. Ω is the interaction parameter in regular-solution theory and x the Ge fraction. For Ω, we use the value of 9 meV/atom, obtained from first-principles calculations [18]. $\bar{U}$ is the elastic energy as expressed in Eq. (1) with the strains in the substrate and island region modified to read $e_s = \kappa(z - z_0) + x_s e_m$ and $e_i = \kappa(z - z_0) + x_i e_m$ in order to account for intermixing. x_s and x_i are the Ge fractions in the substrate and island regions, respectively, obeying to the relation $x_s = \frac{f}{1-f}(1 - x_i)$, where f is the fraction of the number of atoms in the island. Also, the elastic constants C_s and C_i are modified to account for alloying, and are given as linear interpolations of the elemental values according to the Vegard's law.

By assuming full configurational entropy, we model the case where the system is allowed to reach its thermodynamic equilibrium state. The alloy follows ideal mixing, thus the change in entropy, ΔS, is given by

$$\Delta S = fk_B[x_i \ln(x_i) + (1-x_i)\ln(1-x_i)] + (1-f)k_B[x_s \ln(x_s) + (1-x_s)\ln(1-x_s)]. \qquad (4)$$

However, in most cases of interest, when short times are available during device processing, nonequilibrium effects and processes are dominant. These effects arise from kinetic limitations due to high diffusion barriers [9,19], coupled to various geometrical factors [20,21] related to diffusion in the bulk, at and near surface layers, island facets, corners, edges and trenches, etc. We capture such effects within our constrained equilibrium analysis in a generic way, without incorporating the details of the atomistic processes involved, by varying the contribution of ΔS to the free energy from lower values, corresponding to strongly kinetically limited intermixing and suppression of intraisland bulk diffusion, to progressively higher values leading to the full equilibrium state.

Given these concepts, and assuming that interdiffusion and bending can occur simultaneously, the Ge fraction in the island and the value of the curvature are calculated by minimizing the free energy with respect to x_i and κ. The results of this analysis in terms of the relative thickness β are shown in Fig. 4. A number of striking conclusions can be drawn from this analysis. On the left, we see that when both modes of stress relaxation are operating the induced curvature is smaller, compared to the case where no intermixing is allowed, for all values of β. Furthermore, minimizing the entropy contribution leads to maximum bending.

On the right, we see that the Ge fraction in curved islands is always higher compared to flat islands. The effect is small

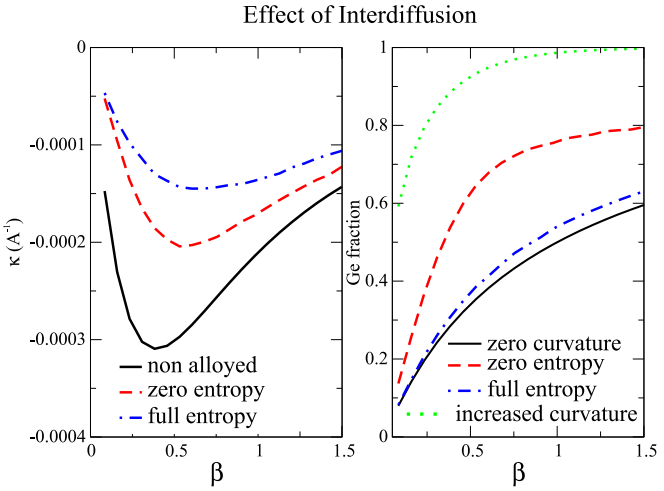

FIG. 4. (Left) Bending as a function of β in nonalloyed (solid line) and in alloyed SOI structures for the two extremes of entropic mixing. (Right) The Ge fraction as a function of β in alloyed SOI structures compared to the flat case. Dotted line describes Ge fraction with full entropy (unconstrained diffusion) under large curvature ($\kappa = -3 \times 10^{-2}$ nm^{-1}) conditions. "Zero entropy" is the limiting case of constrained diffusion, used to highlight the upper bound in the Ge content of the island. In the limit $\beta \to 0$, the island disappears, so the Ge fraction becomes zero, while for $\beta \gg 1$, the substrate disappears leading to a system composed of 100% Ge.

for $\beta \ll 1$, i.e., for very small islands, when the Ge fraction diminishes and the role of curvature becomes unimportant. This is the case where the island elastic energy contribution is minimal. However, for a system like SOI where film and substrate thicknesses are comparable, this contribution becomes significant and the induced curvature drives to higher Ge fractions compared to the flat case. The effect is pronounced in kinetically limited conditions where entropic mixing is reduced. Even higher Ge fractions can be achieved by fixing the curvature to large values (see dotted line in Fig. 4). This situation may be closely relevant to cases where Ge islands are grown on patterned structures with high curvatures, such as stripe ridges and mesa edges [22].

C. Diffusion model and kinetic effects

A more rigorous treatment of kinetic effects can be obtained through a 1D kinetic diffusion model that was developed by us earlier [23] in order to study the diffusion of Ge in Ge/Si(001) dislocated structures. This model yields not only the average Ge fraction in the whole island but also the Ge fraction, averaged laterally, as one moves from the basal plane vertically to the top. The key element in this model is the equation for the diffusion currents for the two species,

$$j = -M(\nabla\mu_a - \nabla\mu_b), \tag{5}$$

where μ_a and μ_b are the chemical potentials for each element. The $\mu's$ are functionals of the Ge fraction x, which is now a function of time and position. Assuming that no voids are formed, the continuity equation, $\partial x(z,t)/\partial t = -\nabla j$, can be iteratively solved in order to yield the final Ge CP from any initial condition (see Appendix).

The results of the application of this kinetic model are summarized in Fig. 5. The computed CP, under kinetically limited conditions expressed by suppressing ΔS by 85%, is given for both a flat island and for curved islands with increasing values of the curvature. Also given for comparison

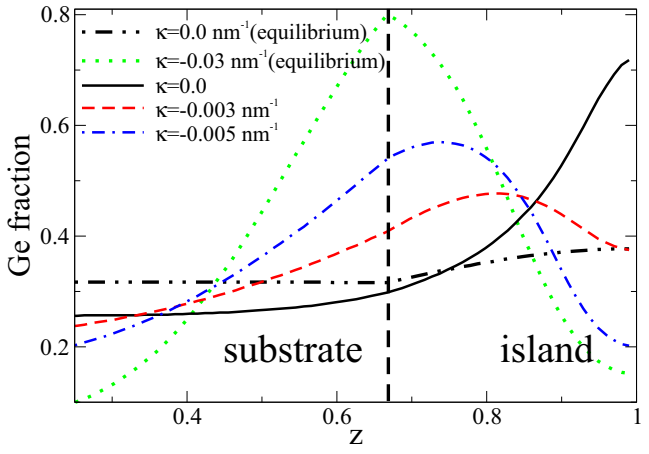

FIG. 5. The Ge fraction (CP) along the axial direction (z axis) from a kinetic diffusion model. The z axis is in relative units. The entropy of mixing is suppressed by 85% and the Ge fraction is plotted for flat ($\kappa = 0$) and curved islands. Also shown are CPs under equilibrium conditions.

are the CPs for a flat and curved island under full equilibrium conditions.

Let us first note the difference between the equilibrium and the kinetically limited CP of the flat structure. Although these model CPs do not show the lateral variations and do not include the kinetics of the island growth, they roughly reproduce the well known experimental result that the CP in islands grown at near-equilibrium conditions [10] (including intraisland diffusion) and the CP in islands grown at kinetically limited conditions [15] (mainly surface diffusion) are different. A more rigorous 3D atomistic simulational treatment of this problem in both cases, revealing the detailed shape of the CPs as they grow, was given elsewhere [9].

Now, let us compare the CPs of the flat and curved islands. In the flat case ($\kappa = 0$), Ge on average enriches the upper regions of the island (more under kinetically limited conditions, see also Refs. [9,11,15]) while Si enriches the bottom. As curvature is gradually introduced, this is reversed: Ge is depleted from the upper regions and is concentrated in the lower ones, while Si segregates to the top. This is in excellent agreement with the results of the MC simulations as summarized in the graph of Fig. 1). Also, the kinetic model clearly predicts that bending leads to the suppression of intermixing and drastically limits the outdiffusion of Ge into the Si thin film, thus strengthening the efficiency of the quantum dots. The values used for κ are comparable with the experimentally observed values in SOI systems.

IV. CONCLUSIONS

In conclusion, we have demonstrated that the effect of curvature can dramatically alter the composition state of alloyed heteroepitaxial systems. We have studied Ge nanoislands on top of a thin Si layer, such as those resulting from SOI, where the elastic energy partitioning between substrate and island is comparable. Based on Monte Carlo simulations and analytic modeling, we observe that both the shape of the composition profile and the Ge content of the island are strongly affected. The presence of curvature can reduce alloying in the system, particularly when kinetic effects are important. This is the first time where these two effects, local bending and interdiffusion, are coupled together. This methodology is general and can be applied to other similar heteroepitaxial systems.

ACKNOWLEDGMENTS

This work is supported by the Strategic Infrastructure Project NEW INFRASTRUCTURE/ΣΤΡΑΤΗ/0308/04 of DESMI 2008, which is co-financed by the European Regional Development Fund, the European Social Fund, the Cohesion Fund, and the Research Promotion Foundation of the Republic of Cyprus. We acknowledge computation time provided by the Cy-Tera facility of the Cyprus Institute under the project CyTera (NEW INFRASTRUCTURE/ΣΤΡΑΤΗ/0308/31).

APPENDIX

In this appendix, more information is given regarding the compatibility of free energy minimization with the

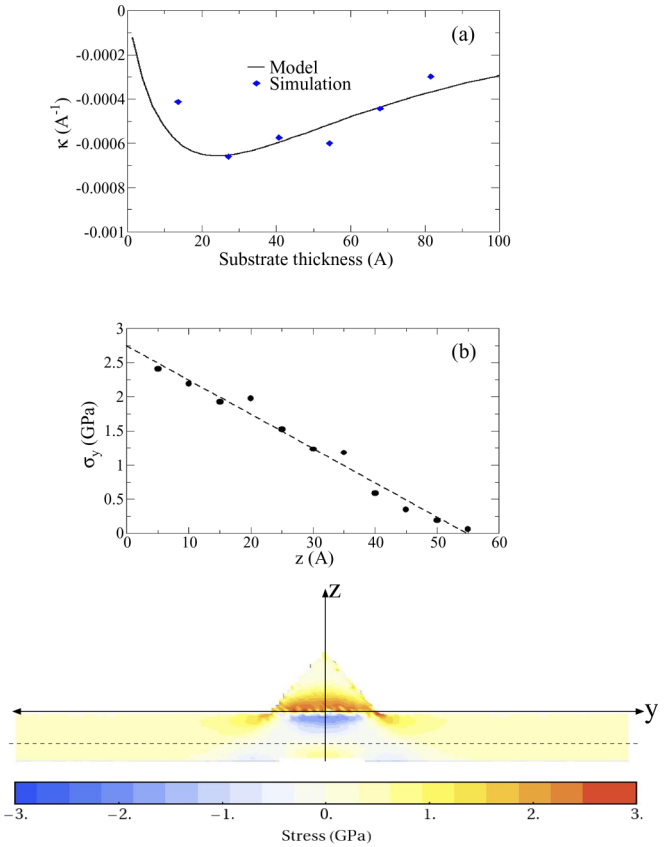

FIG. 6. The contour plot of the biaxial stress component, σ_y. The broken line indicates the position of the neutral plane. Two graphs are also included (a) the value of the curvature from Eq. (2) of the paper (solid line) compared with the value obtained from the Monte Carlo simulations after energy minimization. A 60-nm high pyramid was used and the curvature was measured for various values of the substrate thickness. (b) The biaxial stress component as a function of the island height (z).

methodology of Liu *et al.* [2]. More information on the kinetic model is also provided.

An equation for the curvature was derived in Ref. [2] [Eq. (2)], where the key ingredient was the minimization of the elastic energy. In graph (a) of Fig. 6, we compare the curvature resulting from our Monte Carlo (MC) simulations with this equation. There is an excellent agreement between the two. In graph (b) of Fig. 6, we plot the average biaxial stress component, from the base to the top of the pyramid. The biaxial stress is linearly decreasing from a maximum at the base of the pyramid to a zero value at the top. Such a linear variation was also used in modeling the elastic energy [Eq. (1)]. In addition, we show the stress profile of the biaxial stress component, σ_y,

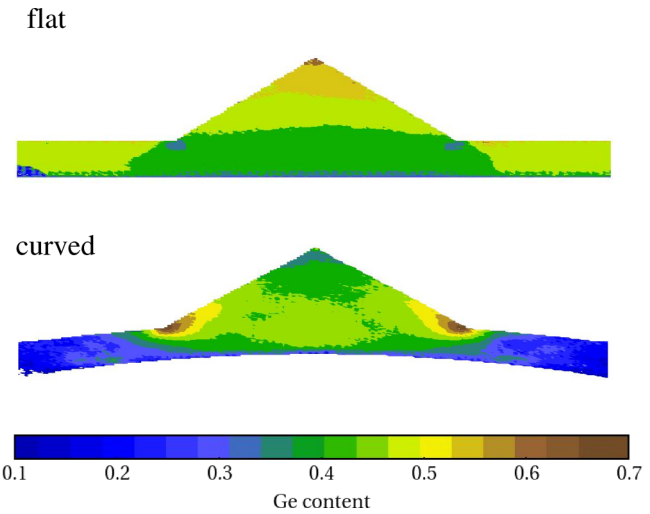

FIG. 7. The Ge composition profile of a SiGe pyramid on SOI for flat and curved ($\kappa = -5 \times 10^{-3}$ nm^{-1}) substrates.

for the entire structure where the position of the neutral plane is identified.

We now give some more details about the kinetic model used in our work and developed earlier in Ref. [23]. Assuming that no voids form, we have equal and opposite diffusion currents for the two species, obeying

$$j = -M(\nabla\mu_a - \nabla\mu_b), \tag{A1}$$

$$M = \frac{m_b x_b m_a x_a}{m_a x_a + m_b x_b}. \tag{A2}$$

Here, m_a and m_b are the elemental mobilities, x_a and x_b are the respective concentrations, and μ_a and μ_b are the chemical potentials for each element, calculated numerically from the gradient of the free energy [Eq. (3)]. For simplicity, we assume $m_a = m_b$, so that $M = x(1-x)m$, where x is the Ge fraction. In general, m may itself depend on composition and on stress but these dependencies are expected to be small corrections to the effects discussed here, so we omit any such dependence.

We obtain the spatial and time evolution of the composition by solving, through discretization, the continuity equation $\partial x(z,t)/\partial t = -\nabla j$, with the flux given by Eq. (A1). The application of the above model is described in the main article where it is evident that by reducing the entropic contribution the degree of alloying is also reduced. For comparison, Fig. 7 illustrates this phenomenon through Monte Carlo simulations. For a fixed value of curvature, we show the Ge fraction of a quantum dot on top of a SOI substrate with comparable thickness. It is evident from the CP that intermixing with the Si template is highly suppressed in the presence of curvature.

[1] F. Liu, P. Rugheimert, E. Mateeva, D. E. Savage, and M. G. Lagally, Nature (London) **416**, 498 (2002).
[2] F. Liu, M. Huang, P. P. Rugheimer, D. E. Savage, and M. G. Lagally, Phys. Rev. Lett. **89**, 136101 (2002).
[3] P. G. Evans, D. S. Tinberg, M. M. Roberts, M. G. Lagally, Y. Xiao, B. Lai, and Z. Cai, Appl. Phys. Lett. **87**, 073112 (2005).
[4] M. Huang, P. Rugheimer, M. G. Lagally, and F. Liu, Phys. Rev. B **72**, 085450 (2005).

[5] M. M. Roberts, L. J. Klein, D. E. Savage, K. A. Slinker, M. Friesen, G. Celler, M. A. Eriksson, and M. G. Lagally, Nat. Mater. **5**, 388 (2006).
[6] F. Cavallo and M. G. Lagally, Nanoscale Res. Lett. **7**, 628 (2012).
[7] A. M. Smith and S. Nie, Acc. Chem. Res. **43**, 190 (2010); M. Virgilio and G. Grosso, J. Phys. Condens. Matter **18**, 1021 (2006).
[8] J. R. Snchez-Prez, C. Boztug, F. Chen, F. F. Sudradjat, D. M. Paskiewicz, R. B. Jacobson, M. G. Lagally, and R. Paiella, Proc. Natl. Acad. Sci. USA **108**, 18893 (2011).
[9] C. Georgiou, T. Leontiou, and P. C. Kelires, AIP Adv. **4**, 077135 (2014).
[10] A. Malachias, S. Kycia, G. Medeiros-Ribeiro, R. Magalhaes-Paniago, T. I. Kamins, and R. S. Williams, Phys. Rev. Lett. **91**, 176101 (2003).
[11] G. Medeiros-Ribeiro and R. S. Williams, Nano Lett. **7**, 223 (2007).
[12] P. C. Kelires and J. Tersoff, Phys. Rev. Lett. **63**, 1164 (1989).
[13] P. C. Kelires, Phys. Rev. Lett. **75**, 1114 (1995).
[14] G. Hadjisavvas and P. C. Kelires, Phys. Rev. B **72**, 075334 (2005).
[15] U. Denker, M. Stoffel, and O. G. Schmidt, Phys. Rev. Lett. **90**, 196102 (2003).
[16] J. Tersoff, Phys. Rev. B **39**, 5566 (1989).
[17] J. Stangl, V. Holý, and G. Bauer, Rev. Mod. Phys. **76**, 725 (2004).
[18] J. L. Martins and A. Zunger, Phys. Rev. Lett. **56**, 1400 (1986).
[19] X. B. Niu, G. B. Stringfellow, and F. Liu, Phys. Rev. Lett. **107**, 076101 (2011).
[20] J. B. Hannon, M. Copel, R. Stumpf, M. C. Reuter, and R. M. Tromp, Phys. Rev. Lett. **92**, 216104 (2004); N. Paul, S. Filimonov, V. Cherepanov, M. Çakmak, and B. Voigtländer, *ibid.* **98**, 166104 (2007).
[21] P. Sonnet and P. C. Kelires, Appl. Phys. Lett. **85**, 203 (2004).
[22] B. Yang, F. Liu, and M. G. Lagally, Phys. Rev. Lett. **92**, 025502 (2004).
[23] T. Leontiou, J. Tersoff, and P. C. Kelires, Phys. Rev. Lett. **105**, 236104 (2010).